Available online at www.sciencedirect.com
SCIENCE DIRECT®
Polymer 45 (2004) 3091–3098
polymer
www.elsevier.com/locate/polymer

Tacticity distribution of isotactic polypropylene prepared with heterogeneous Ziegler–Natta catalyst. 1. Fractionation of polypropylene

Ville Virkkunen[a,*], Pasi Laari[a], Päivi Pitkänen[b], Franciska Sundholm[a]

[a]*Laboratory of Polymer Chemistry, University of Helsinki, P.O. Box 55, Helsinki FI-00014, Finland*
[b]*Borealis Polymers Oy, P.O. Box 330, Porvoo FI-06101, Finland*

Received 4 December 2003; received in revised form 2 February 2004; accepted 25 February 2004

Abstract

Two polypropylene samples, one with relatively low isotacticity and the other with high isotacticity were fractionated using a series of solvents and temperatures. For both samples 4–9 fractions were collected and characterised with differential calorimetry, size exclusion chromatography and ^{13}C NMR spectroscopy. The collected fractions showed typical characteristics of a fractionation based on isotacticity, but also similarities to results from temperature rising elution fractionation (TREF), even though a separate controlled crystallisation step was not used. The melting temperatures of the fractions were found to increase linearly as a function of the *meso* diad fraction. A calibration, which can be used to convert DSC melting curves to wt% curves of isotacticity, was constructed for the temperature range 108–165 °C. The calibration enables quick analysis of samples in polypropylene manufacturing processes.

Keywords: Polypropylene; Fractionation; Isotacticity

1. Introduction

It is well recognized that heterogeneous Ziegler–Natta catalysts contain multiple active sites, which produce polypropylene (PP) with varying degree of stereoregularity. Despite considerable efforts with different analysis methods, it has not been possible to determine the exact structures of the highly reactive active sites. Recently, some progress has been achieved with molecular modelling methods [1–3], but more common is an indirect approach to study the polymer structure. If the polymer characterisation can be done thoroughly enough, information on the catalyst is gained as well. The most revealing information related to the catalyst and the polymerisation mechanism of polypropylene is the distribution of stereoerrors and stereoregular sequences in the formed polymer. This fine structure also determines for most part of the mechanical properties, such as stiffness of the material. Recently, Viville et al. [4] showed that changes in the mechanical properties of PP are not only due to differences in the average isotacticity but also in the way tacticity is distributed between the chains. Clearly, average properties are not sufficient for the characterisation of the complex polymer structure produced with heterogeneous Ziegler–Natta catalysts [5].

Currently the only quantitative method for determining the distribution of stereodefects in PP comprises fractionation of the polymer and a separate analysis of the fractions. This is extremely time consuming and tedious work. An alternative method is analytical temperature rising elution fractionation (TREF) [6], which is the most common method for obtaining qualitative information about the chemical composition of polymers. In TREF the sample is first crystallised slowly on a column from a dilute solution and then eluted from it, while raising temperature. The result is a fractogram of the eluted polymer as a function of the elution temperature. The method has been used mainly with polyolefins like polyethylene, ethylene copolymers [6,7] and polypropylene [8], but also with random copolyester [9,10]. Results have been correlated with short chain branching and comonomer content.

The fractionation mechanism in TREF is based on the longest crystallisable sequence [4,9,10]. The longest sequences, not interrupted by branch points or comonomers

* Corresponding author. Tel.: +358-919-150-338; fax: +358-919-150-330.
E-mail address: ville.virkkunen@helsinki.fi (V. Virkkunen).

0032-3861/$ - see front matter © 2004 Elsevier Ltd. All rights reserved.
doi:10.1016/j.polymer.2004.02.060

that cannot enter the lamellar structure, determine the highest crystallisation temperature of a chain. When the temperature is lowered during the crystallisation phase in TREF, the chains with the longest sequences are the first to form thermodynamically stable crystals and segregate. Upon further lowering of the temperature, on top of the first crystallites, a second layer is formed from chains with the second longest crystallisable sequences. The third and following layers are formed in similar fashion. According to this scheme, the distribution of the regular sequences along the chain does not influence the fractionation. TREF gives information only about the inter-chain distribution of the longest crystallisable sequence. When applied to polypropylene, this means that the distribution of the longest isotactic sequence is determined.

High solvent consumption and time consuming crystallisation steps in TREF have motivated the development of new compensating methods. Among these are CRYSTAF [12] and calorimetric methods SIST (stepwise isothermal segregation technique) [13,14] and SSA (Successive Self-nucleation and Annealing) [15]. In CRYSTAF, the elution step of TREF is skipped by measuring the change in concentration of the solution directly during the cooling phase. According to Beigzadeh et al. [11] the fractionation in CRYSTAF is also based on the longest crystallisable sequence of the chain.

In calorimetric DSC methods, the analysis is based on the subsequent melting behaviour of the samples after controlled crystallisation. For best results, Wild et al. [16] used solution-crystallisation, but similar results can also be obtained with pure samples and controlled thermal treatments, such as SIST and SSA. If the molecular segregation during the crystallisation is successful, the remaining difference between the melting curve and TREF fractogram is due to dependence of the heat capacity C_p on crystallinity. Because of this, the melting curve is not mass-dependent like the corresponding TREF fractogram. To correct this difference it is possible to construct a calibration with samples of varying crystallinity and narrow tacticity distribution [16].

The main advantage of DSC methods, besides the shorter measurement times, is the additional information, which is obtained from the polymer structure. If shorter sequences along the chain have crystallised, they will also contribute to the melting curve [17]. With calorimetric methods, it should thus be possible to analyse the intra-molecular distribution of crystallisable sequences.

Both SIST and SSA have been applied to the study of copolymers and short chain branching [13,15], but not widely to the analysis of PP. From these two methods, SSA has enhanced resolution in copolymer analysis. It also seems promising for PP, because the crystallisation is performed at elevated temperatures. According to Maiti et al. significant numbers of crosshatches are not formed when the crystallisation temperature is above 150 °C [18]. Crosshatches are undesirable in molecular fractionation of PP, because they are formed at later stages of the crystallisation and are therefore grown into the constraining framework of the radial lamella [19–21].

The objective of this study is to investigate possibilities for analysing the tacticity distribution of isotactic polypropylene using SSA in combination with a calibration. In the present work the preparation and characterisation of polypropylene fractions with narrow tacticity distributions is reported. The fractions are used to construct a calibration, which is needed to convert a melting curve to a mass dependent curve. This work is a continuation of our previous work [14] on modelling propene polymerisation. Analysis of the fractions also allows for a more detailed study on the effect of the catalyst (electron donors) on the distribution of the stereodefects. In the second part of this study [22] the applicability of the SSA method for the analysis of polypropylene structure is studied and compared to the well established TREF.

2. Experimental

2.1. Materials

Two polypropylene bench scale homopolymer samples (A and B) from Borealis Polymers Oy were used in this study. Preparation of the samples follows the description given in reference [14]. For these samples Al/Do (triethylaluminium/dicyclopentyldimethoxysilane) ratio was 10 and 200, respectively.

2.2. Solvent fractionation

Several studies and methods for fractionation of isotactic polypropylene have been published over the years [8,23–27]. For this study, a method based on the use of hydrocarbon solvents with increasing solvent power was selected.

Before the fractionation, samples were homogenised by dissolving about 13.5 g of the sample in hot xylene (800 ml) and then precipitating with acetone (2000 ml). Fractionation of the homogenised samples was performed in two stages. First, the whole sample was divided into octane soluble (OS) and insoluble fractions (OI) in 80 °C and then these fractions were divided further according to the following procedure.

Fractionation of the OS part was performed in *n*-pentane (25 and 35 °C) and in *n*-hexane (45 and 60 °C), so that five fractions could be collected. Fractionation was performed by stirring the solvent (45 ml)–polymer mixture in the desired temperature for 2 h and then separating the solvent and the insoluble polymer using a combination of hot-centrifugation and hot-filtration.

Fractionation of the OI part was performed in glass vessel (1 l), which was equipped with a Lauda thermostat and a vibrostirrer. 400 ml of the solvent was preheated to the

desired temperature and added to the vessel containing the polymer above a steal net and a thin layer of glass wool. Fractionation time was 30 min after which the solvent was run to a decanter from a tap in the bottom of the glass vessel and the next solvent was added. The fractionation was performed under nitrogen blanketing. The collected fractions were precipitated with acetone (400 ml), filtrated and left to dry for 2 days. 1 g/l of Irganox 1010 was used as an antioxidant in the solvents of the homogenisation and OI fractionation phase. The first part of the fractionation was performed twice for sample B to get enough material for the ^{13}C NMR measurements.

2.3. XS

The amount of xylene soluble material at 25 °C (XS) was measured by dissolving a known amount of polypropylene in boiling xylene according to ISO 6427 (1992). After cooling to room temperature, the insoluble fraction was filtered off and the solution was evaporated to dryness.

2.4. TREF

The composition distributions of the polymers were obtained using analytical temperature rising elution fractionation. The TREF profiles were generated using an instrument built in-house (Borealis Polymers Oy) according to a published design [6,7]. The samples were dissolved in xylene (about 2 mg/ml) at 135 °C and injected into the column at 135 °C and the latter was then cooled to 15 °C at a rate of 1.5 °C/h. The column was subsequently eluted with 1,2,4-trichlorobenzene (TCB) at a flow rate of 0.5 ml/min while the temperature was increased from 20 to 140 °C over 5 h. The output, detected with an IR detector operating at a wavelength of 3.41 μm, was presented as a fractogram normalized to constant area.

2.5. DSC

All differential scanning calorimetry (DSC) measurements were performed with a Mettler 822e differential scanning calorimeter in a nitrogen atmosphere. Samples of about 3 mg in aluminium pans were first melted by heating over the temperature range 30–225 °C, then cooled to 30 °C and then remelted over the temperature range 30–225 °C. Heating and cooling were done at a rate of 10 °C/min. Melting temperature and crystallinity were determined from the second melting. The degree of crystallinity was calculated by comparison with heat of fusion (dH_f) of a perfectly crystalline polypropylene, i.e., 209 J/g [28].

2.6. GPC

The molar masses and molar mass distributions of the samples were determined at 135 °C on a Millipore Waters 150C ALC/GPC instrument. Two mixed bed and one 10^7 Å TSK-Gel columns were applied and the solvent used was 1,2,4-trichlorobenzene. The calibration was made according to a universal calibration method using narrow distribution polystyrene standards and narrow and broad polypropylenes.

2.7. NMR

NMR measurements were performed with Varian ^{UNITY}INOVA 300 MHz NMR spectrometer operating at 75.47 MHz for carbon. 240 mg samples (when possible) were dissolved in 1.5 ml of 1,2,4-trichlorobenzene with 10% DMSO-d_6 in 10 mm NMR tubes. For the less soluble fractions (5–8) the ^{13}C spectra was recorded at 140 °C. To get better resolution the more soluble samples were measured at 110 °C [29]. All sequences between 19 and 22 ppm were assigned according to Busico et al. [29]. Due to the different solvent (1,2,4-trichlorobenzene with 10% benzene-d_6), the assignments were checked by measuring one sample in both solvents. Experimental conditions were: number of pulses about 10 000, pulse angle 90°, spectrum width 16 000 Hz, relaxation delay 8 s, spinning speed 15 Hz. All spectra were completely proton decoupled.

3. Results and discussion

The samples for the fractionation were chosen so that enough material could be collected for the whole tacticity scale. With modern Z–N catalysts, it is difficult to obtain significant amounts of PP with low isotacticity. Because of this, the second sample was adjusted to have very low isotacticity. The xylene soluble amount (XS%) of sample B is 15.0% compared to the 1.2% of sample A. The difference of the samples is clearly seen in their TREF fractograms (Fig. 1). For both samples, the major part of the polymer is eluted at over 110 °C. The peak value for sample B is, however, about 10 °C lower and the peak is significantly broader. This indicates a much broader tacticity distribution

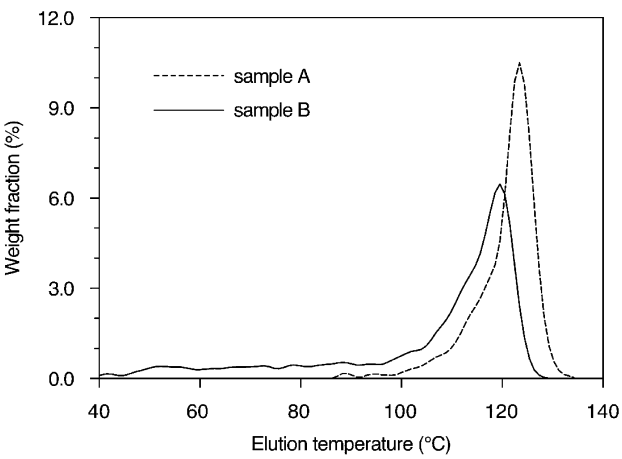

Fig. 1. TREF fractograms of the polypropylene samples A and B.

and shorter isotactic sequences. The fractogram of sample B also has a very long low temperature tail. The difference in the elution temperature of the least isotactic material of the samples is over 40 °C.

If the fractionation proceeded according to isotacticity, the wt% of the fractions should qualitatively follow the TREF fractograms of the whole samples. This is evident in the fractionation results (Table 1 and Fig. 2). Over 70 wt% of the sample A was obtained in only one fractionation step (A8) and the part of sample A that was soluble in octane at 80 °C (A5) was just over 1 wt%. Because of the low amount of this fraction, it could not be fractionated further. For sample B, on the other hand, the long low temperature tail is obvious in the much larger octane soluble fraction (almost 15 wt%), which could be divided further into 5 fractions (B1–B5). The total amount of the octane (80 °C) soluble material correlates well with the measured XS values of the samples.

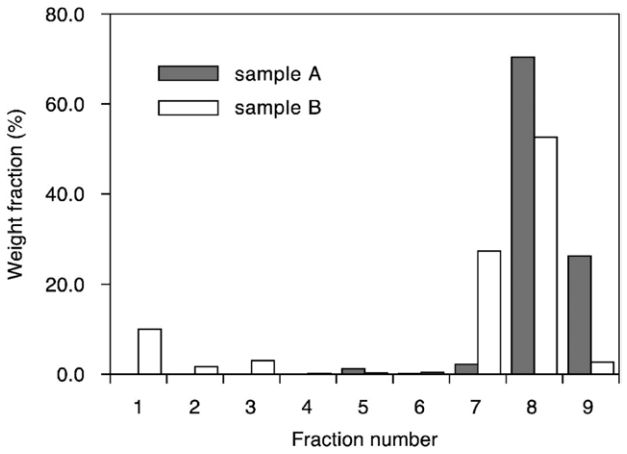

Fig. 2. Weight fractions (%) of the polypropylene fractions. Note that the fraction 5 of sample A (octane 80 °C) was not fractionated further.

3.1. Thermal analysis of the fractions

For the calibration, it is important that the melting temperatures of the fractions cover a wide temperature range. Table 1, Figs. 3 and 4 show the results of the thermal analysis of the fractions. For the less isotactic sample B the octane soluble fractions show almost linearly increasing melting temperatures from 108 to 137 °C. In the less soluble fractions B6–B9 the peak temperature is much more constant around 160 °C. In case of sample A, only the two last fractions have similar melting temperatures. For these fractions the peak temperatures are found 2.6–3.8 °C higher than for sample B. The total melting temperature range is 108–165 °C, which is sufficient for the calibration of typical isotactic polypropylene samples.

The increasing trend and even spacing of the T_m values in the fractionation series indicates that the fractionation was successful and fractions with narrow tacticity distribution have been obtained. However, according to Burfield et al. [30], crystallinity (dH_f) is a better measure of isotacticity than T_m. As shown in Fig. 4 the crystallinities of the fractions do not increase as linearly in the series as do the T_m values. This means that the fractions have been separated, not according to average isotacticity, but according to lamellar thickness or the lengths of the crystallisable sequences in the chains. The result is then very similar to what is obtained in TREF, even though separate controlled crystallisation step was not used. The similarity is also seen if the crystallinity values of the two series are compared. For a given solvent–temperature pair, crystallinity is consistently higher in the fractions of sample A (except A5, which cannot be compared with the other fractions). Viville et al. [4] obtained very similar results in a preparative TREF study of two isotactic polypropylene samples. Both of the analysed samples had isotacticity over 97%, but the more isotactic one had consistently higher isotacticity (*mmmm*%) (and $\bar{M}_w$) in the fractions collected at the same temperature.

In solvent fractionation, there is also the possibility that molar mass has influenced the fractionation. Based on the similar crystallinities of the last fractions, a difference in molar mass could also explain the separation of these fractions.

Table 1
Results from the solvent fractionation of the polypropylene samples and from the thermal analysis of the fractions

Fraction	Solvent	Temperature (°C)	Sample A			Sample B		
			wt%	T_m (°C)	Cryst. (%)	wt%	T_m (°C)	Cryst. (%)
1	Pentane	25				10.0	–	–
2	Pentane	35				1.7	107.8	12.8
3	Hexane	45				3.0	123.4	25.2
4	Hexane	60				0.2	128.4	28.7
5	Octane	80	1.2	124.7	22.1	0.3	136.6	26.6
6	Toluene	75	0.1	137.0	34.6	0.4	159.6	26.8
7	Toluene	94	2.2	149.5	51.9	27.4	156.3	46.2
8	Xylene	112	70.4	163.8	52.8	52.6	161.2	47.7
9	Xylene	127	26.3	165.2	49.8	2.7	161.4	48.5

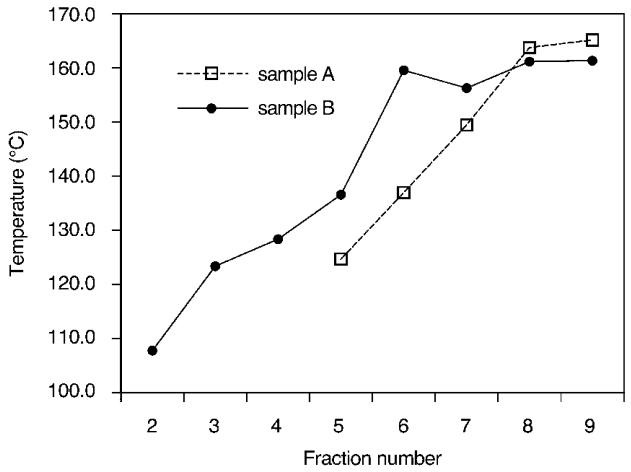

Fig. 3. Melting temperatures of the polypropylene fractions determined with differential calorimetry.

3.2. GPC analysis

Table 2 lists the results for the GPC analysis of the fractions. Fig. 5(a) and (b) show the GPC results of the original samples along with the weighted GPC curves of the fractions and their sums. In both cases, more than 98% of the original samples were collected in the fractions. This is shown in the good correspondence of the GPC curve of the unfractionated samples and the sum of the GPC curves of the fractions. For the more isotactic sample (A), $\bar{M}_w$ is clearly higher and the distribution is narrower, but for both A and B the polydispersities are still relatively high (7.6 and 12.2, respectively).

The GPC data of the fractions are plotted in Fig. 6. For both series, there is a strong increase in the number average molar masses ($\bar{M}_n$) of the higher temperature fractions. This result could be interpreted to mean that these fractions were mainly separated according to molar mass. Fractionations based on molar mass, however, typically yield fractions with very narrow molar mass distributions. As shown in Table 2 the less isotactic fractions have very broad distributions (>4.6). For the more isotactic fractions, the distributions become narrower, but for the last fractions, the values are still close to 4. These values are comparable to the results of the preparative TREF study [1] and typical for a tacticity-based

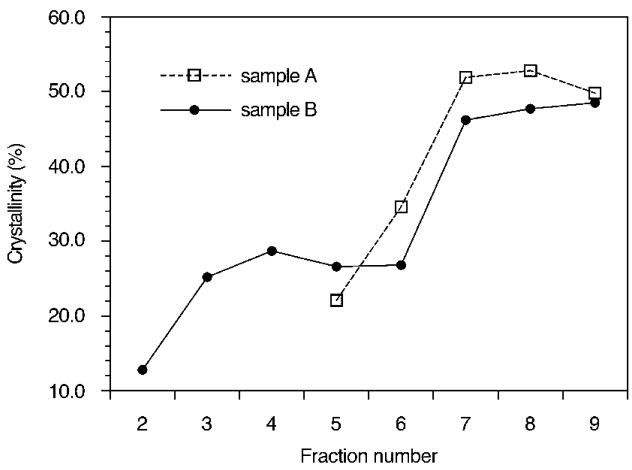

Fig. 4. DSC determined crystallinities of the polypropylene fractions.

Table 2
Number and weight average molar masses and polydispersities of the polypropylene fractions and unfractionated samples A and B

Fraction	Sample A			Sample B		
	$\bar{M}_w$	$\bar{M}_n$	$\bar{M}_w/\bar{M}_n$	$\bar{M}_w$	$\bar{M}_n$	$\bar{M}_w/\bar{M}_n$
1				55 400	4990	11.1
2				40 000	5500	7.3
3				42 000	6030	7.0
4				40 200	8840	4.6
5	61 400	6750	9.1			
6				73 500	11 100	6.7
7	18 800	6300	3.0	116 000	29 200	4.0
8	277 000	68 700	4.0	227 000	61 200	3.7
9	376 000	88 600	4.2	224 000	61 100	3.7
Unfractionated	331 000	43 700	7.6	131 000	10 400	12.6

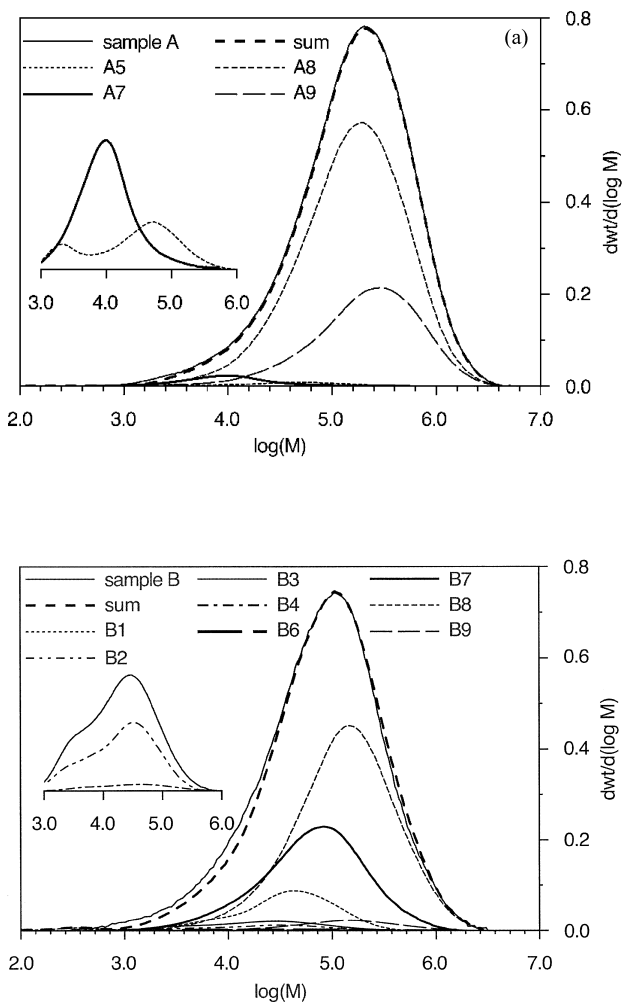

Fig. 5. Molar mass distributions of samples A and B with the weighted distributions of the fractions and their sum. Distributions of the smaller fractions (A5, A7 and B2–B4) are shown on the left with a magnified scale.

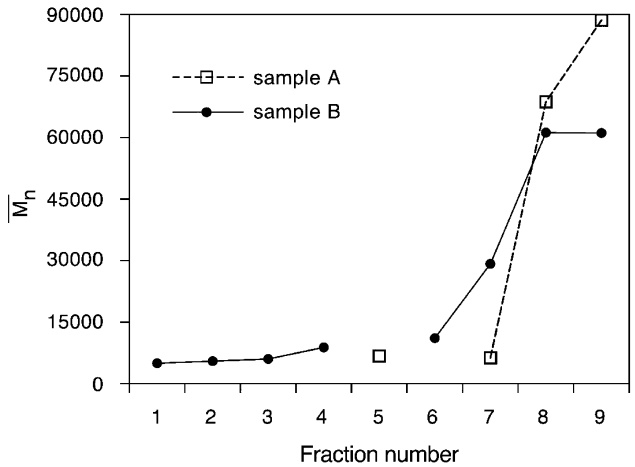

Fig. 6. $\bar{M}_n$ values of the polypropylene fractions.

fractionation. Same conclusion can also be drawn from Fig. 7, which shows crystallinity as a function of $\bar{M}_n$. The trend is similar to the results in previous tacticity-based fractionations [27].

The broad molar mass distributions indicate that all fractions (A5–A9, B1–B9) contain polymer produced by several site types. Vice versa this means that polymer from one site is distributed on several fractions. This is seen especially clearly from the molar mass distributions of the octane soluble fractions (Fig. 5). These distributions are bimodal, with the same two peaks occurring in all four fractions. The fact that polymer from one site is distributed in four fractions means that this site produces polymer with very broad tacticity distribution. According Soares et al. [5] this is exactly what can be expected based on the statistical nature of the polymerisation. The distribution of tacticity becomes broader for the sites producing lower average molar mass.

From the two peaks of the octane soluble fractions, the higher molar mass peak appears to be the one corresponding to the most atactic material in the polymer. In the room temperature soluble fraction (B1), this peak is the dominating one and the lower molar mass peak is practically non-existing. The lower molar mass peak probably comprises the low molar mass material from the more isotactic sites. Comparison of the octane soluble fractions of sample A and B reveals that the modification of the catalyst (Al/Do 200 → 10) has almost completely deactivated the site responsible for the atactic polymer (B1). Both the bimodal shape of the distribution and the crystallinity values indicate that the small A5 fraction corresponds more to the hexane soluble fractions of sample B than to the B1 fraction.

For the octane 80 °C insoluble fractions there does not appear to be any correspondence in the molar masses between the samples. Both A8, A9 have significantly higher $\bar{M}_w$ than any of the B fractions.

3.3. ^{13}C NMR results

The detected pentad sequence intensities for the fractions are listed in Table 3. The fraction of *meso* pentad in the series is presented in Fig. 8. The results effectively reproduce the crystallinity results. Together with the molar mass values there are, however, some peculiar points. In the A7 and B7 fractions, the *mmmm%* values are almost identical, but the number average molar mass $\bar{M}_n$ is clearly higher for the fraction B7. For A8 and B8 the values are the other way around: $\bar{M}_n$ values are of the same order of magnitude, but A8 is significantly more isotactic than B8. The only explanation for these seemingly inconsistent results is that, like in TREF, also in this case the longest crystallisable sequences have determined the fractionation. The result then verifies the earlier assumption. In both cases (A7, B7 and A8, B8), the crystallisable sequences must be of the same order, despite the large difference in chain lengths or the average defect content. This means that not only the inter-molecular, but also the intra-molecular distribution of tacticity is much broader in sample B. This information is obtainable only by fractionation of the samples. It provides good support for the three-site model that some of us put forth recently [14]. The difference in the

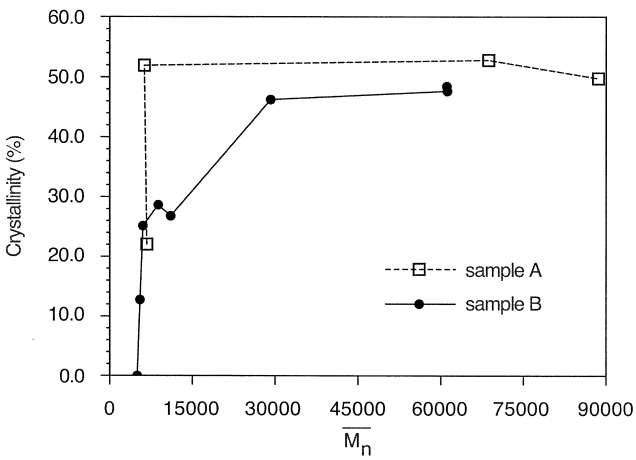

Fig. 7. Crystallinities of the polypropylene fractions as a function of the number average molar mass ($\bar{M}_n$).

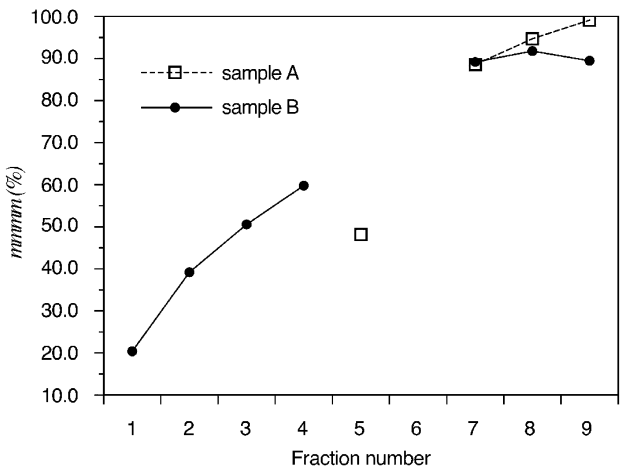

Fig. 8. Isotacticities (*mmmm%*) of the polypropylene fractions.

Table 3
Results from the ^{13}C NMR analysis of the polypropylene fractions

Fraction	*mmmm* (%)	*mmmr* (%)	*rmmr* (%)	*mmrr* (%)	*mmrm* + *rmrr* (%)	*rmrm* (%)	*rrrr* (%)	*rrrm* (%)	*mrrm* (%)
A5	48.2	10.7	2.6	12.0	6.6	1.0	8.7	5.2	5.1
A7	88.5	3.2	0.3	2.9	1.9	0.2	0.4	0.9	1.2
A8	94.7	2.1	0.9	1.2	0.8	0.0	0.0	0.0	0.3
A9	99.1	0.6	0.1	0.2	0.0	0.0	0.0	0.0	0.0
B1	20.4	10.1	5.4	15.9	12.6	1.7	15.6	10.6	7.7
B2	39.2	10.9	3.7	14.2	7.4	1.4	9.8	7.2	6.1
B3	50.6	9.9	0.9	9.6	5.2	0.5	13.4	3.7	6.3
B4	59.8	8.9	3.2	8.5	4.6	1.0	5.7	4.0	4.3
B7	89.2	3.7	0.2	3.5	0.7	0.0	0.3	0.8	1.6
B8	91.8	2.3	0.4	2.1	1.7	0.1	0.2	0.4	1.1
B9	89.5	4.1	0.7	2.7	0.7	0.2	0.4	0.6	1.2

isotacticity between fractions A7–A9 and B7–B9 is well explained with the shift in the donor equilibrium reaction. Also the change in the molar mass is most notable in these fractions in accordance with the change in the donor equilibrium.

The broad tacticity distribution of B is also seen in the pentad intensities. Even the most isotactic fractions of sample B contain the atactic pentads *mrmr*, *rmmr* and *rrrm*. The existence of these pentads indicates that the stereo-defects are found in blocky structures as reported previously [26,29]. Only small amount of the *rmmr* pentad is detectable in the A8 and A9 fractions.

3.4. Calibration

In Fig. 9, the *meso*-diad fraction (*m*) is represented as a function of the melting temperatures of the fractions. The linear fit to the experimental points is excellent. It is also remarkable how well the two lines (for A and B) coincide especially when it is considered that the molar masses of the fractions differ significantly. Burfield et al. [30] have reported that when different kinds of Ziegler–Natta polypropylenes are compared, enthalpy of fusion is a good measure of isotacticity. They found an equation of the form log(ΔH) vs. log(*mm*) to give the best linear fit for several different polypropylenes (both fractions and whole samples). If log(ΔH) vs. log(*mm*) is plotted for our data, an excellent linear fit is obtained.

The line in Fig. 9 basically allows for the conversion of the DSC curve to a tacticity distribution. Considering the results of Burfield et al. [30] it is, however, only safe to use this calibration with samples polymerised with similar catalysts. As discussed previously, before the conversion, the change in heat capacity (C_p) due to different degrees of crystallinity has to be corrected. For poly(ethylene-*co*-1-butene) fractions, Wild et al. plotted the value of $\Delta H_{max}/\Delta H_T$ as a function of the melting temperatures [16]. This curve is plotted in Fig. 10 along with the curve derived by Wild et al. for comparison. Using this calibration, a DSC measurement can be converted to correspond to the fractogram obtained from TREF. As is the case for poly(ethylene-*co*-1-butene), also for polypropylene the fraction of the material in the low temperature region (< 150 °C) is underestimated in DSC measurements. Due to

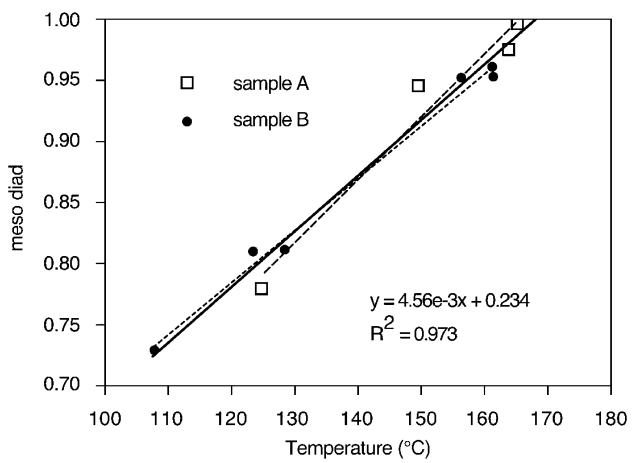

Fig. 9. *meso*-Diad fraction of the collected polypropylene fractions as a function of the melting peak values. Dashed lines: linear fits for A and B, solid line: linear fit for both A and B.

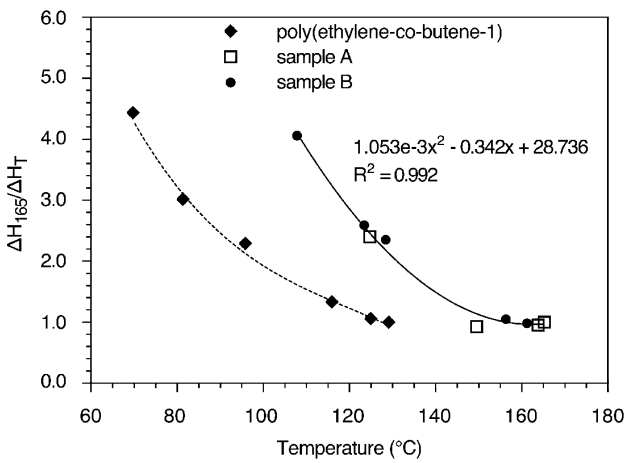

Fig. 10. $\Delta H_{165}/\Delta H_T$ ratio, calculated from the differential calorimetry results of the polypropylene fractions, plotted as a function of the melting temperature. Data for poly(ethylene-*co*-1-butene) are from Ref. [16].

the higher melting temperature of PP, the curve is shifted to higher temperatures.

The remaining problem in the determination of the tacticity distribution for polypropylene is due to the complex crystallisation behaviour of polypropylene. In the second part of this study, the use of the successive self-nucleation and annealing measurement will be evaluated.

4. Conclusions

In this work, two polypropylene samples were fractionated using a series of temperatures and solvents with increasing boiling points. In the first four fractions the chosen temperatures and solvents performed extremely well and a series of fractions with narrow melting peaks and an even temperature gap between the peaks was obtained. The major part of the samples was collected in the last three fractions. In these, more isotactic fractions also the molar mass increased drastically. The molar mass distributions, however, remained broad, which indicates that the separation was mainly due to tacticity differences. The controlling factor was, however, not the average isotacticity, but the lengths of the crystallisable isotactic sequences. This was shown by the different isotacticities of the fractions extracted with a particular solvent at a set temperature.

The use of additional solvents or smaller temperature intervals in the second part of the fractionation would have allowed for the collection of smaller fractions, but even with the current fractionation scheme, the melting peaks of the fractions were relatively narrow. This indicates that the fractions had narrow tacticity distribution and were suitable for the calibration. The correlation between isotacticticity (*meso* diad) and the melting peaks of the fractions was linear in the whole melting temperature interval 108–165 °C. The $\Delta H_{max}/\Delta H_T$ calibration was constructed with excellent fitting constant ($r^2 > 0.99$) and can thus be used to convert a DSC melting curve of polypropylene samples made with similar catalyst systems to a mass dependent curve.

With respect to the effect of the electron donor in the polymerisations of the samples A and B, it is clear that the site responsible for the atactic material is deactivated almost completely by the external electron donor. In addition, both the molar mass and isotacticity of the isotactic fractions increased and their distributions became narrower. The 15-fold decrease of the octane soluble fraction was the combined result of these effects. All these results support well the recently published qualitative model of the propene polymerisation with a Ziegler–Natta catalyst.

Acknowledgements

We thank Dr A. Lehtinen for helpful discussions during the work.

References

[1] Boero M, Parrinello M, Hüffer S, Weiss H. J Am Chem Soc 2000;122:501.
[2] Cavallo L, Guerra G, Corradini P. J Am Chem Soc 1998;120:2428.
[3] Virkkunen V, Pietilä L-O, Sundholm F. Polymer 2003;44:3133.
[4] Viville P, Daoust D, Jonas AM, Nysten B, Legras R, Dupire M, Michel J, Debras G. Polymer 2001;42:1953.
[5] Soares JBP. Chem Engng Sci 2001;56:4131.
[6] Wild L. Trends Polym Sci 1993;1:50.
[7] Wild L, Ryle T, Knobeloch D, Peat I. J Polym Sci, Polym Phys Ed 1982;20:441.
[8] Xu J, Feng L, Yang S, Yang Y, Kong X. Eur Polym J 1998;34:431.
[9] Lodefier P, Daoust D, Jonas AM, Legras R. Macromol Symp 1999;148:59.
[10] Lodefier P, Jonas AM, Legras R. Macromolecules 1999;32:7135.
[11] Beigzadeh D, Soares JBP, Duever TA. J Appl Polym Sci 1999;80:2200.
[12] Monrabal B. Macromol Symp 1996;110:81.
[13] Chen F, Shanks RA, Amarasinghe G. Polymer 2001;42:4579.
[14] Garoff T, Virkkunen V, Jääskeläinen P, Vestberg T. Eur Polym J 2003;39:1679.
[15] Müller AJ, Hernández ZH, Arnal ML, Sánchez JJ. Polym Bull 1997;39:465.
[16] Wild L, Chang S, Shankernarayanan MJ. Polym Prepr 1990;31:270.
[17] Gabriel C, Lilge D. Polymer 2001;42:297.
[18] Maiti P, Hikosaka M, Yamada K, Toda A, Gu F. Macromolecules 2000;33:9069.
[19] Janimak JJ, Cheng SZD, Giusti PA, Hsieh ET. Macromolecules 1991;24:2253.
[20] Zhu X, Yan D, Tan S, Wang T, Yan T, Zhou E. J Appl Polym Sci 2000;77:163.
[21] Weng J, Olley RH, Bassett DC, Jääskeläinen P. J Macromol Sci Phys 2002;B41:891.
[22] Virkkunen V, Laari P, Pitkänen P, Sundholm F. Polymer, submitted.
[23] Ogawa T, Hoshino S. J Appl Polym Sci 1973;17:2235.
[24] Kawamura H, Hayashi T, Inoue Y, Chûjô R. Macromolecules 1989;22:2181.
[25] Paukkeri R, Iiskola E, Lehtinen A, Salminen H. Polymer 1994;35:2636.
[26] Paukkeri R, Väänänen T, Lehtinen A. Polymer 1993;34:2488.
[27] Lehtinen A, Paukkeri R. Macromol Chem Phys 1994;195:1539.
[28] Brandrup J, Immergut EH. Polymer handbook, 3rd ed. Wiley: New York; 1989. p. V/2.
[29] Busico V, Cipullo R, Monaco G, Talarico G, Vacatello M, Chadwick JC, Segre AL, Sudmeijer O. Macromolecules 1999;32:4173.
[30] Burfield DR, Loi PST, Doi Y, Mejzik J. J Appl Polym Sci 1990;41:1095.